

Article

Study of Renewable Energy Penetration on a Benchmark Generation and Transmission System

Oluwaseun M. Akeyo , Aron Patrick  ‡, and Dan M. Ionel 

SPARK Laboratory, ECE Department, University of Kentucky, Lexington, KY, USA

‡ Louisville Gas and Electric and Kentucky Utilities, Louisville, KY, USA

* Correspondence: dan.ionel@ieee.org

Version January 6, 2021 submitted to *Energies*

Abstract: Significant changes in conventional generator operation and transmission system planning will be required to accommodate increasing solar photovoltaic (PV) penetration. There is a limit to the maximum amount of solar that can be connected in a service area without the need for significant upgrades to the existing generation and transmission infrastructure. This study proposes a framework for analyzing the impact of increasing solar penetration on generation and transmission networks while considering the responses of conventional generators to changes in solar PV output power. Contrary to traditional approaches in which it is assumed that generation can always match demand, this framework employs a detailed minute-to-minute (M-M) dispatch model capable of capturing the impact of renewable intermittency and estimating the over- and under-generation dispatch scenarios due to solar volatility and surplus generation. The impact of high solar PV penetration was evaluated on a modified benchmark model, which includes generators with defined characteristics including unit ramp rates, heat rates, operation cost curves, and minimum and maximum generation limits. The PV hosting capacity, defined as the maximum solar PV penetration the system can support without substantial generation imbalances, transmission bus voltage, or thermal violation was estimated for the example transmission circuit considered. The results of the study indicate that increasing solar penetration may lead to a substantial increase in generation imbalances and the maximum solar PV system that can be connected to a transmission circuit varies based on the point of interconnection, load, and the connected generator specifications and responses.

Keywords: Hosting capacity, photovoltaic, PSS/E, economic dispatch, voltage violations, thermal limits, PV penetration, solar

1. Introduction

Renewable energy resources are rapidly becoming an integral part of electricity generation portfolios around the world due to declining costs, government subsidies, and corporate sustainability goals. Large renewable installations on a transmission network may have potential impacts on the delivered power quality and reliability, including voltage and frequency variations, increased system losses, and higher wear of protection equipment [1]. Estimating the maximum hosting capacity of a transmission network may be used to determine the highest renewable penetration the system can handle without significant violations to the quality of the power delivered and the reliability of the grid.

Most recent literature has been focused on analyzing the impact of intermittent renewables on either generation or transmission systems only [2–5]. In [6], a methodology for estimating the solar PV hosting capacity based on steady-state circuit violations, without a detailed economic dispatch model was proposed. Typical dispatch models in literature assume generation can always match load or set optimization constraints that are only acceptable for hourly dispatch models with relatively low



Figure 1. The aerial view of the E.W. Brown generating station, which includes Kentucky's largest solar farm, hydropower plant, natural gas units, and coal fired power plants.

35 load variations [7–9]. These hourly dispatch models may not be suitable for capturing the impact of
36 PV systems for practical generation service areas, which record generation imbalance violations over
37 duration as low as 15-minutes.

38 Furthermore, a substantial portion of literature has been focused on estimating the maximum PV
39 hosting capacity for distributions systems and proposing network configurations that do not consider
40 the contributions of conventional generators [10–13]. However, more than 60% of PV installations in
41 the US are utility-scale setups typically connected to the transmission network [14]. Steady-state and
42 transient analysis of transmission networks were presented in [6,15], but none of the works considered
43 the variability of the connected loads or present a detailed economic dispatch to capture the responses
44 of the conventional generators.

45 This research presents a framework for analyzing the impact of increasing PV penetration on both
46 generation and transmission systems. Contrary to conventional approaches dispatching units with
47 substantial intermittent renewable resources with hourly-based dispatch models[16,17], this approach
48 employs an M-M dispatch model capable of capturing the impact of large solar PV penetration and
49 identifying minute-based periods of generation imbalance due to PV volatility and surplus power.
50 The presented technique is also capable of analyzing the impact of increasing PV system penetration
51 have on transmission circuits while considering the responses of conventional generators to changes
52 in solar PV power.

53 The impact of increasing solar PV penetration was analyzed on a modified IEEE 12 bus system
54 [18] with generators, including coal, natural gas combustion turbine (NGCT), natural gas combined
55 cycle (NGCC), and a hydropower plant with practical unit specifications. This study uses generator
56 models developed on data provided by LG&E and KU on operational units to simulate the responses
57 of conventional generators to increasing solar PV penetration (Figure 1). Publicly available one-minute
58 irradiance data for the 10MW PV farm located at the utility's facility was used to model typical
59 variation in solar irradiance [19]. The PV hosting capacity of the example generation and transmission
60 network systems analyzed was estimated based on voltage, thermal, and generator dispatch violations.

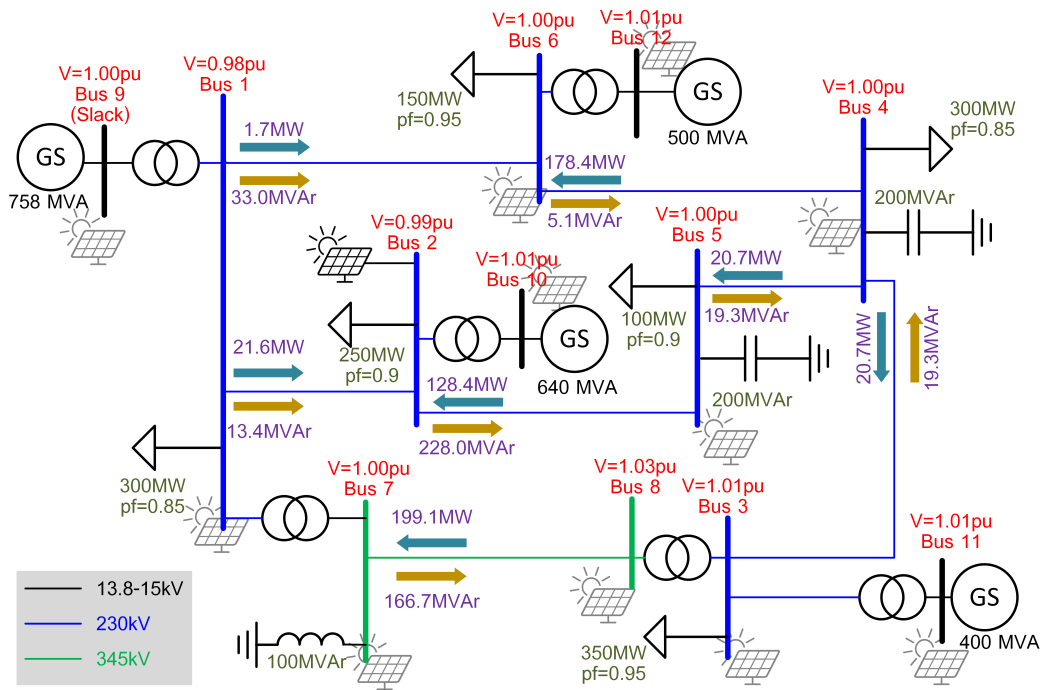


Figure 2. Single line diagram for the modified benchmark network with PV plant connected to bus 2 and values corresponding to approximately 65% (1450MW) load level. The transmission circuit was completely assessed for PV connection at any of its buses.

2. Proposed minute-to-minute economic dispatch model

The real-time changes in load from minute to minute are relatively minimal due to aggregation. However, the volatility of the net demand on conventional thermal generators rises significantly with the increase in intermittent renewable energy penetration. While it is nearly impossible to always match generation with demand for a service area, utilities are penalized by regulators for generation imbalances lasting longer than acceptable minutes [20,21]. Hence, conventional hourly dispatch models are not suitable to identify the generation imbalances and effectively capture the effect of solar PV intermittency on evaluated service area.

This approach employs a minute-based dispatch since the solar PV power variability due to cloud cover is expected to reduce as the plant capacity and footprint increases. The proposed minute-to-minute dispatch model in this study was developed for the IEEE 12 bus test system illustrated in Figure 2. The system which consists of four generating units was modified based on the specifications presented in Table 1 and subjected to realistic load variations for an example day in the Fall season. The efficiency of thermal generating units in terms of their heat rate vary with percentage output for different types of units (Figure 3). In this approach, the heat rates for thermal units is described as follows:

$$Q_g^R(P_g) = \frac{Q_g^{in}(P_g)}{P_g} \approx a_g P_g^2 + b_g P_g + c_g, \quad (1)$$

where, $Q_g^R(P_g)$ represents the heat rate for unit g with output power P_g ; Q_g^{in} the heat requirement; and a_g, b_g, c_g are the heat rate co-efficient of the generator. Therefore, the operating cost for each unit may be expressed as:

$$C_g(P_g) = Q_g^R(P_g) \cdot F_g + Z_g, \quad (2)$$

where, C_g is the running cost for generator g ; F_g , the fuel cost and Z_g , the fixed cost constant, which includes maintenance and emission reduction costs. Therefore, the proposed M-M dispatch model is

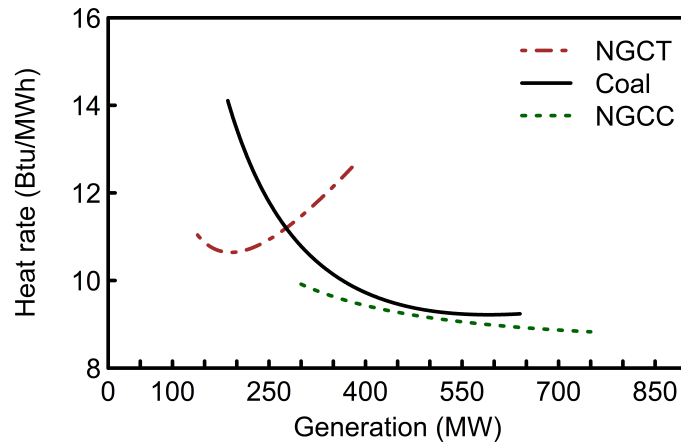


Figure 3. Example heat rate curve for natural gas combustion turbine (NGCT), coal, and natural gas combined cycle (NGCC) thermal generators considered in this study.

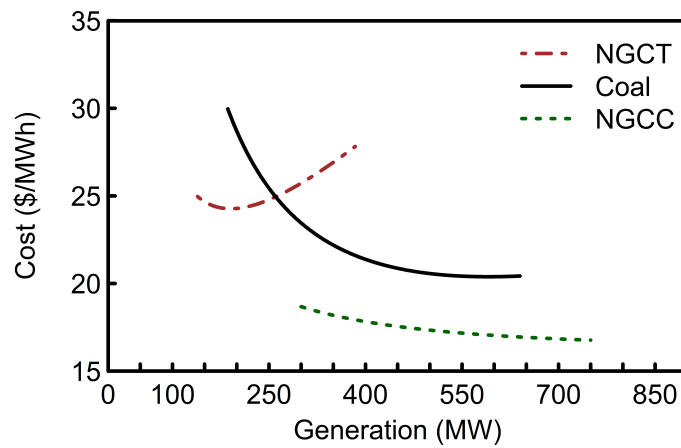


Figure 4. The operation cost in \$/MWh including the fuel and auxiliary costs for the thermal units considered. The cost rate in \$/h can be calculated as a product of the operation cost and the generation.

79 capable of estimating the running cost of the thermal units for specified output level within its limits
80 of operation (Figure 4).

For a practical economic dispatch problem, the objective is to minimize cost and generation imbalance such that the cheapest combination of generators are regulated to meet demand. Therefore, the economic dispatch model objective can be expressed as:

$$\min \begin{cases} C_T = \sum_{g=1}^G C_g(P_g) \\ \epsilon = |P_T - L_c| \end{cases}, \quad (3)$$

Table 1. Specifications for the generating units in the modified IEEE 12 bus test case studied

Bus no	Type	Rating [MW]	Min gen [MW]	Ramp [MW/min]	Heat rate co-eff.			Fuel [\$/MMBtu]	Aux [\$/MWh]
					a[10 ⁻³]	b	c		
9	NGCC	750	368	10	0.4	7.7	630	1.76	1.23
10	Coal	640	288	7	5.5	2.7	1935	1.96	1.79
11	NGCT	384	203	9	20.7	2.7	753	1.76	5.54
12	Hydro	474	-	-	-	-	-	-	-

where,

$$P_T = P_1 + P_2 + \dots + P_G, \quad (4)$$

C_T , represents the total operating cost for all units considered; P_T , the combined generator output; L_c , the combined service area load; and G the total number of operational units including the PV plant. Following theoretical developments in [22], the minimum C_T for each instance without considering generator constraints and transmission losses occurs when the total differential cost is zero and may be described as follows:

$$\partial C_T = \frac{\partial C_T}{\partial P_1} dP_1 + \frac{\partial C_T}{\partial P_2} dP_2 + \dots + \frac{\partial C_T}{\partial P_G} dP_G = 0. \quad (5)$$

81 However, due to generator constraints including ramp-rate limitation of units the result from (5) may
82 fall outside operation range.

Contrary to conventional approaches, this approach recognizes the practical limitations of generator units. The constraints for the considered thermal units are as follows:

$$P_g^{min}(t) \leq P_g(t) \leq P_g^{max}(t) \quad (6)$$

$$P_g^{min}(t) = \max \left[\underline{P}_g, P_g(t - \Delta t) - \Delta t \cdot R_g^{down} \right] \quad (7)$$

$$P_g^{max}(t) = \min \left[\overline{P}_g, P_g(t - \Delta t) + \Delta t \cdot R_g^{up} \right] \quad (8)$$

83 where, $P_g^{max}(t)$ and $P_g^{min}(t)$ are the maximum and minimum output power for unit g , respectively;
84 \overline{P}_g and \underline{P}_g are the specified maximum and minimum generator operation limits; R_g^{up} and R_g^{down} , the
85 generator rising and falling ramp rates, respectively.

This study is focused on the impact of increasing PV penetration on an example system with five generators. The proposed framework economic dispatch model employs a multi-objective genetic algorithm (GA) to minimize C_T and ϵ for the three thermal units in the system and the "non-dispatchable" units (PV and hydro) output are set based on reference values from practical modules. The solar plant reference power module was developed based on measured irradiance data retrieved from an operational solar PV farm. The PV output power is expressed as follows:

$$P_{pv} = \frac{\gamma}{1000} \times \eta \times \overline{P}_{pv}, \quad (9)$$

86 where P_{pv} is the PV plant power, γ is solar irradiance in W/m^2 ; η is the inverter efficiency, and \overline{P}_{pv} is
87 the rated capacity. The algorithm goes through multiple combinations of generator set points limited
88 by $P_g^{min}(t)$ and $P_g^{max}(t)$ for each unit to establish a Pareto front. Since the primary objective of the
89 utilities is to meet demand, the design with the least amount of imbalance is selected for the simulation
90 time-step (Figure 5). In order to identify periods of over- and under-generation, the proposed M-M
91 dispatch model assumes the generators in the transmission circuit are solely responsible for meeting
92 demand for the concerned service area without need for off system sales and electricity power trading.
93 Factors such as units commitment and outage are beyond the scope of this study. Therefore, all units
94 are assumed to be available and committed throughout the example day.

95 3. Conventional generators response to increasing PV penetration

96 Increasing solar penetration can make it more challenging for grid operators to balance generation
97 with load in real-time, since generating units are committed based on load forecast and level of
98 uncertainty. In this study, the integrated PV farms are operated in "must-take" modes, in which
99 thermal units are turned down to accommodate solar PV penetration. The relatively high power

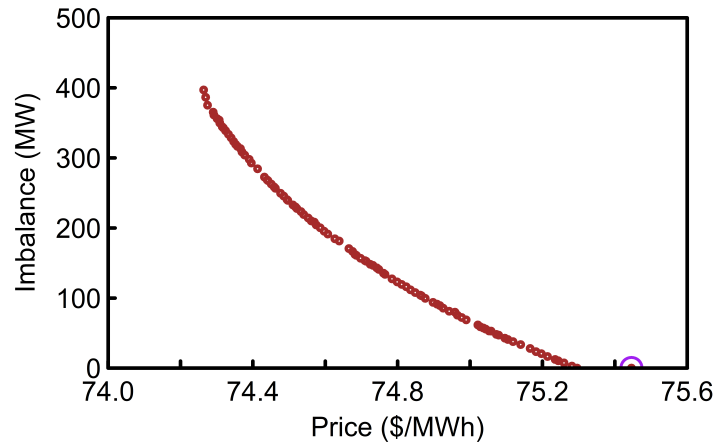


Figure 5. The multi-objective optimization Pareto front for example minute. The selected design is the one with the minimum imbalance for every case.

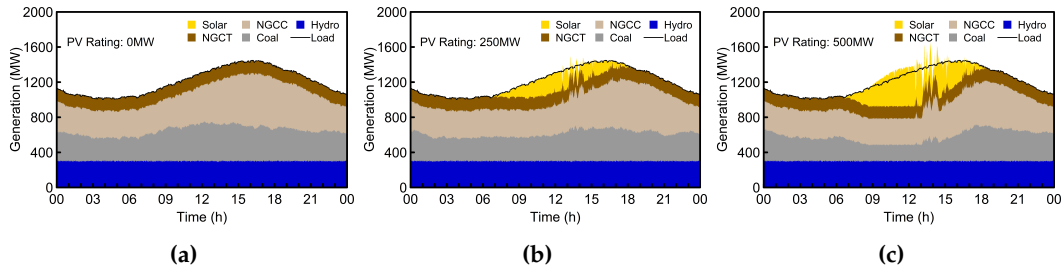


Figure 6. Minute-to-minute (M-M) unit economic dispatch highlighting the impact of increasing PV penetration on an example generation portfolio. The results indicate that large PV penetrations may lead to both over- and under-generation scenarios where combined power from units cannot match demand. The presented analysis include (a) no PV, (b) 250MW PV, and (c) 500MW PV penetration case studies.

100 variation of the PV plant for the example day considered leads to significant generation imbalance
101 during periods when the operating units cannot ramp up or down fast enough to meet demand.

102 Due to the minimum generation limit of the available thermal unit, a significant level of
103 over-generation may be observed at hours between 9:00 and 13:00, when the generators could not
104 ramp down further to accommodate the increasing PV penetration (Figure 6). In addition to the rest
105 time required to restart thermal units, a significant amount of time, up to 24 hours for some coal units
106 is required to restart start them which makes it extremely challenging to turn off the units at midday
107 and restart them for evening peak [23].

The current solar PV regulatory standards may not be sufficient for managing high intermittent renewable sources penetration and new standards will be required to ensure grid stability in a future grid [24,25]. Furthermore, the penetration of distributed renewable sources such as rooftop solar will lead to substantial changes in the apparent load on the transmission network that may call for additional regulations. In this study, a generation violation or imbalance count is recorded when the area control error, ACE, exceeds ± 20 MW for defined consecutive minutes. The ACE is expressed as:

$$ACE = (T_m - T_s) + \beta_f(f - f_s), \quad (10)$$

where, T_m and T_s are the measured and scheduled tie line lows, f and f_s , the measured and scheduled frequency, and β_f the frequency bias constant for the area. Frequency variation due to generation

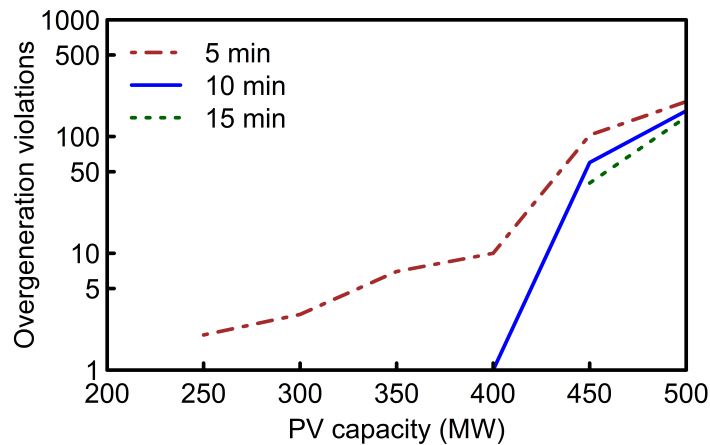


Figure 7. Example day over-generation violation count. In this approach a violation count is recorded when the dispatch imbalance exceeds 20MW over defined consecutive minutes (5, 10 and 15).

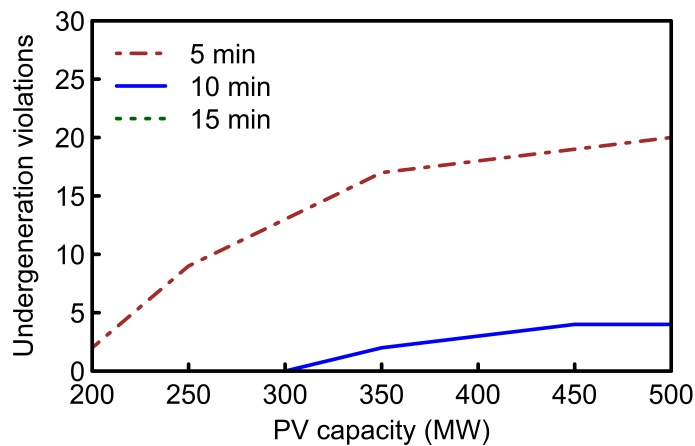


Figure 8. Under-generation violation count at increasing PV penetration rate. Under-generation occurs when PV becomes suddenly shaded and thermal units cannot ramp up fast enough to supply deficit power.

imbalance is beyond the scope of this study, therefore it was assumed that $f = f_s$, and T_s is always equal to zero. Hence, for this analysis (10) can be re-written as:

$$ACE = T_m = P_T - L_c. \quad (11)$$

108

109 The over- and under-generation imbalance count for the example day was evaluated for increasing
 110 PV penetration. A significant level of over-generation can be observed at solar PV penetration levels
 111 exceeding 400MW (Figure 7). This is mainly due to the inability of the available units to operate at
 112 values below their minimum generation limits during periods of surplus solar generation. For the
 113 example day analyzed, there was no under-generation violation lasting more that 15 consecutive
 114 minutes (Figure 8). However, significant under-generation violation counts for 5 and 10 consecutive
 115 minutes, which was relatively constant for PV penetration above 350MW was recorded. These
 116 violations are primarily due to the intermittent behavior of the PV systems and generating units not
 117 being able to ramp fast enough to supply deficit power due to sudden shading of the solar panels.

118 Solar power curtailment can be an effective tool for managing over-generation, in which the
 119 solar PV plant output may be held back when there is insufficient demand to consume production.
 120 This study examined how much curtailment will be required to address solar over-generation for

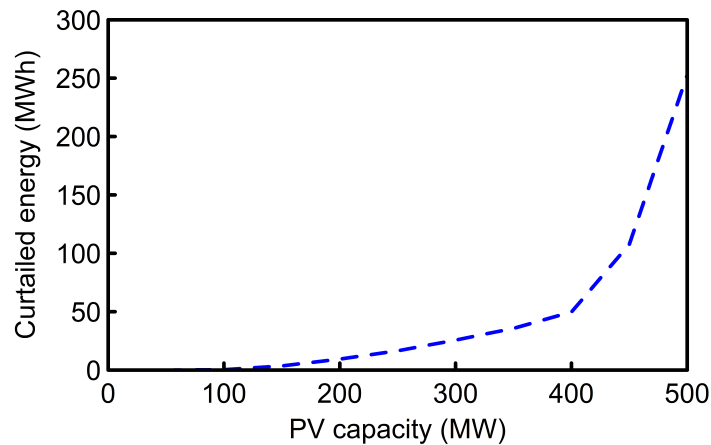


Figure 9. Curtailed energy solar energy for example day. In order to limit over-generation, an exponential increase in the total solar PV power curtailed can be observed.

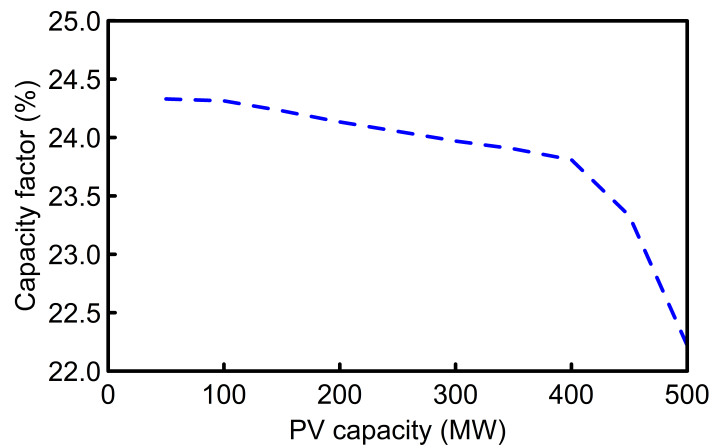


Figure 10. PV plant capacity factor based on penetration. Capacity factor can be observed to reduce with increase in curtailed power.

121 the presented generator portfolio over the example day (Figure 9). An exponential increase in the
 122 curtailed PV energy in order to avoid over-generation violations was recorded, with rapid increase
 123 in curtailment for PV capacity above 400MW. Due to the substantial PV energy curtailed, over 2%
 124 reduction in PV capacity factor was reported at 500MW penetration level (Figure 10). Increase in
 125 solar PV penetration is expected to lead to significant reduction in running cost without considering
 126 the capital cost for the PV system. It is however important to recognize that, PV penetration may
 127 lead to more aggressive usage of fast ramping units such as NGCTs, which are typically the most
 128 expensive units in generation portfolios. This study evaluated the cost savings for the example day
 129 due to increase in PV penetration. A somewhat steady increase in cost savings was reported for solar
 130 PV penetration above 80MW (Figure 11). However, due to generator commitment and increased
 131 operation of the NGCT unit for managing the solar PV variation over the example day, no cost savings
 132 was recorded for solar PV penetration below 80MW.

133 4. Modified benchmark transmission network

134 The modified benchmark transmission system analyzed in this work represents a small islanded
 135 power system network with 12 buses and four generating units (Figure 2). This modified transmission
 136 network is based on the generic 12-bus test system developed for wind power integration studies

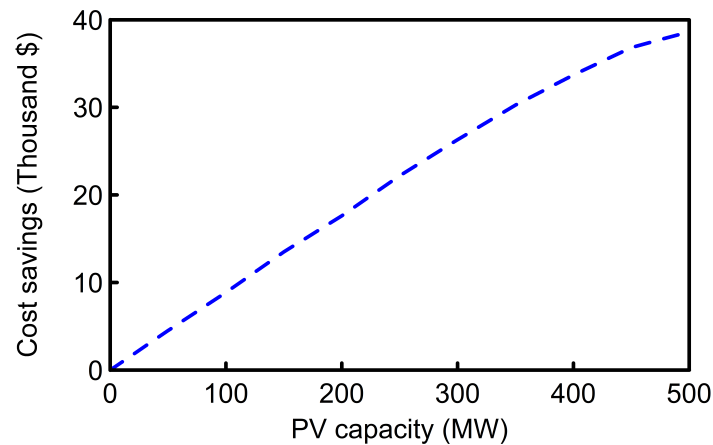


Figure 11. Operation cost saving due to increase in PV penetration. For the example day considered, an increase in operation cost was observed for PV penetrations below 500MW due to operation of inefficient units to meet demand.

137 presented in [18]. The transmission network base case was developed in PSS®E with a single
 138 transmission line connecting buses 3 and 4, as opposed to the parallel cables in the initial setup.

139 At steady-state without renewable integration, the transmission network total system load is
 140 approximately 65% of the total generation capacity. The bus voltage voltages vary between 0.98pu
 141 to 1.03pu. In this example, each of the transmission lines is rated for a maximum of 250MVA power
 142 flow with the exception of the transmission lines connecting buses 7 to 8 and 3 to 4, which are rated
 143 to 500MVA. At 65% load level without renewable integration, the maximum loading for any of the
 144 transmission lines is 71%, which is the power flow between buses 6 and 4.

145 Solar PV penetration have the maximum impact on generation during periods when load is
 146 relatively low. For transmission networks, maximum PV impact is observed during peak periods,
 147 when load is rather high and transmission lines are near saturation. In this approach, the transmission
 148 network was evaluated for the analyzed example day peak demand and the generating units were
 149 dispatched according with respect to minimum operating cost and solar PV penetration. The
 150 benchmark model was further modified to enable renewable system integration, such that a solar PV
 151 farm may be connected to either of its 12 buses. In order to connect the PV plant to a selected bus, an
 152 additional transformer is introduced to connect the PV plant terminal to the corresponding bus. Based
 153 on typical regulatory requirements, the PV plant is configured to be capable of operating at 0.95 power
 154 factor to support scheduled grid voltage at the point of interconnection (POI) [26].

155 5. Proposed framework for network PV hosting capacity

156 The PV hosting capacity for a transmission network is defined as the maximum solar PV capacity
 157 that may be connected to the system without significant upgrades to its circuit to ensure steady
 158 operation. The maximum hosting capacity of a transmission circuit depends on multiple factors
 159 including the bus voltage variation, thermal limits of the transmission lines, frequency variation, fault
 160 currents as well as regulated factors such as total harmonic distortion and grid codes. This study
 161 focuses on the maximum PV capacity that may be connected to any one of the buses in the example
 162 transmission network without violating the bus voltages or the thermal limits of the circuit branches.

163 The proposed framework established as a combination of modules developed in Python and
 164 transmission case studies in PSS®E, may be employed to estimate the hosting capacity for a defined
 165 transmission network. Opposed to conventional approaches, this framework employs a practical and
 166 detailed economic dispatch model, which defines the output power of all available generating units
 167 based on combined running cost. This dispatch model also respects generator minimum power limit

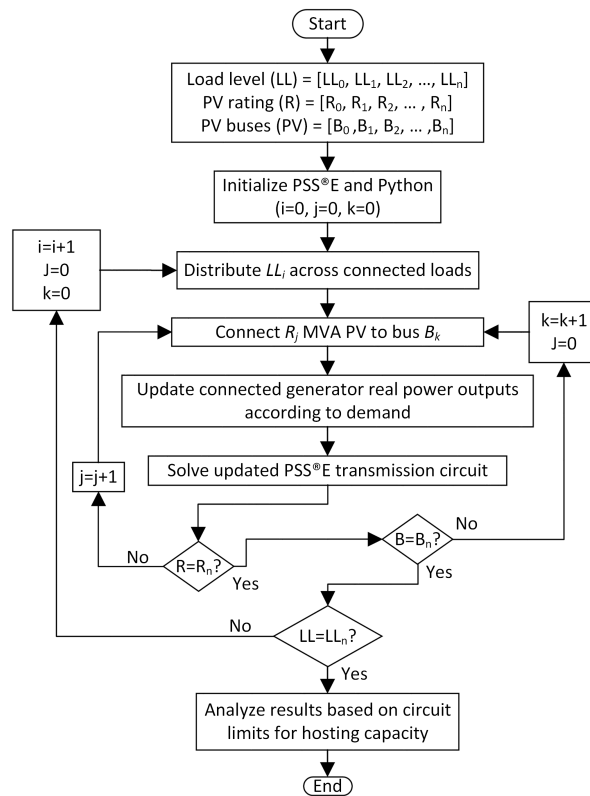


Figure 12. Operational flow chart for the proposed framework for estimating the hosting capacity on a transmission network. The steady state impact for increasing solar PV capacity at different POI was evaluated to estimate the maximum PV hosting capacity for the network.

168 and ensures units are set to values within their operation limits. Hence, the combination of units that
169 meet load at the least cost are dispatched for each case study analyzed.

170 The framework allows the user to define the potential buses for PV connections, the range and
171 maximum PV capacity to be analyzed, and the load levels to be considered. The simulation study is
172 initialized with for the based case without solar PV penetration and the case study is evaluated. The
173 combined load for the analyzed instance is then distributed to all the load buses at a ratio and power
174 factor identical to the base case. The transmission network is then modified such that the minimum
175 PV capacity to be evaluated is connected to the first candidate bus to be analyzed. All the available
176 generators are re-dispatched to accommodate the increase in PV penetration.

177 The modified circuit is solved in PSS®E, and the connected PV rating is increased if the solution
178 converges. The framework keeps increasing the connected PV rating at predefined steps until solution
179 failure or maximum PV rating to be analyzed, after which it resets to a minimum PV rating for the next
180 bus or load level. The simulation comes to an end after the combinations of all PV ratings, connection
181 buses and load levels have been exhaustively tested and results extracted (Figure 12). Based on the
182 criteria defined for the system circuit, the collected results are therefore analyzed to determine the
183 system's maximum hosting capacity.

184 6. Transmission Network Response to Increasing PV Capacity

185 The proposed framework was employed to estimate the PV hosting capacity for the modified IEEE
186 12 transmission network. The PV hosting capacity was evaluated based on the bus voltage responses
187 of the network, thermal loading and circuit solution convergence. The network was evaluated at
188 1450MW combined load level, which represents the peak demand for the example day analyzed. Up
189 to 500MW PV penetration level was analyzed for the defined POI and the operational conventional

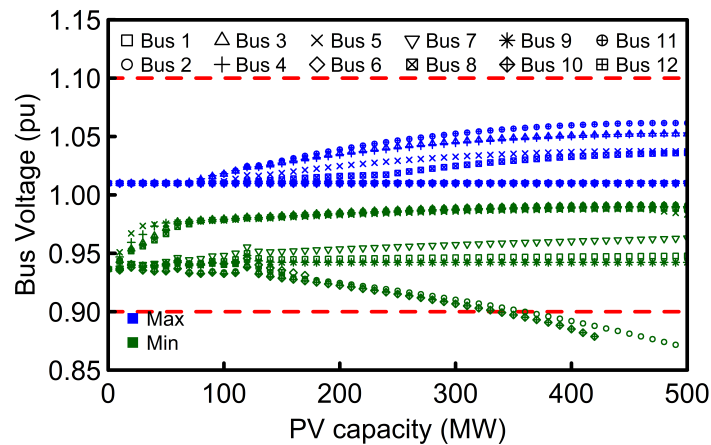


Figure 13. The maximum and minimum bus voltage variation for increasing PV capacity over multiple points of interconnection (POI). A PV capacity is undesirable if it leads to bus voltage variation above 1.1 or below 0.9pu.

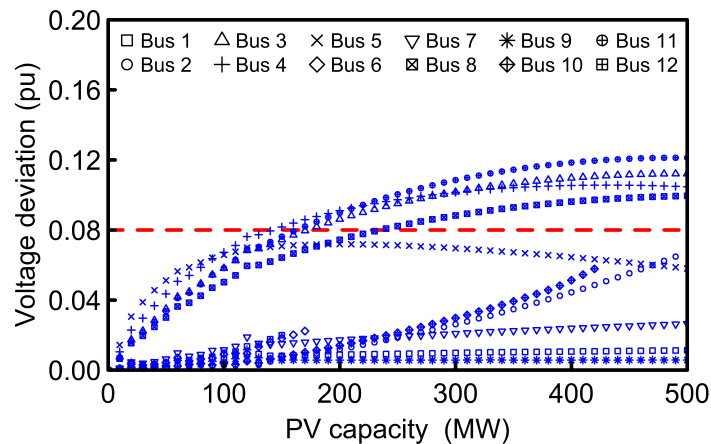


Figure 14. Maximum bus voltage deviation for defined PV capacity. A violation is recorded if the maximum voltage deviation exceeds 0.08pu. The maximum voltage deviation is also an indicator of the expected voltage variation due PV intermittency.

190 generators were re-dispatch for each case to ensure the combination generator output power with the
 191 least cost is selected.

192 Contrary to conventional assumptions, increasing PV penetration does not only lead to increase in
 193 bus voltage. This capability for increasing solar PV capacity to lead to both increase and decrease in bus
 194 voltages was demonstrated in this study. Variations in bus voltage in some cases are due to substantial
 195 changes in power flow, hence significant changes in the voltage drop across the transmission lines.
 196 Utilities are typically regulated to maintain their bus voltages within certain limits, and this study
 197 assumes a violation when any of the bus voltages exceeds 1.1 or below 0.9pu. Due to multiple factors
 198 including substantial circuit violations, networks solutions for PV capacity beyond certain values do
 199 not converge and such cases are only evaluated based on available solutions. The maximum and
 200 minimum bus voltages for the network varies based on the PV POI as illustrated in Figure 13. Hence,
 201 up to 320MW PV capacity can be connected to any of the transmission circuit buses without any
 202 voltage violation.

203 The maximum and minimum bus voltage in a transmission network is significantly influenced
 204 by the scheduled voltages of the connected generator units. Hence, a measure of the maximum and
 205 minimum bus voltages alone may not be able to capture the impact of increasing solar PV penetration.
 206 In addition to the maximum and minimum bus voltage limits, utilities are typically required to

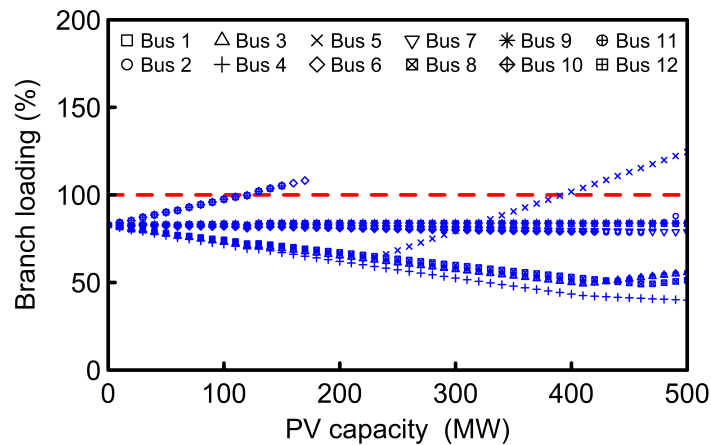


Figure 15. Maximum transmission line loading. Depending on the POI, PV integration may lead to substantial reduction in transmission line loading.

207 maintain bus voltage variation within certain values. This maximum voltage deviation can also be an
 208 indicator of the expected voltage variations due to the PV intermittency. For this study, a PV capacity
 209 that leads to bus voltage deviation that exceeds 0.08pu is undesirable. The maximum voltage deviation
 210 varies based on PV capacity and POI as illustrated in Figure 14. Based on this analysis, up to 140MW
 211 PV may be connected to any of the circuit buses with bus voltage deviations exceeding 0.08pu.

212 Transmission line power flow are typically limited to restrict the temperature attained by energized
 213 conductors and the resulting sag and loss of tensile strength. This study focuses on the maximum
 214 PV penetration the network can sustain at steady state of a substantial period of time. Hence, the
 215 percentage loading for on all the transmission lines were evaluated for defined solar PV capacity.
 216 A thermal violation is recorded when the maximum transmission line loading exceeds 100% of its
 217 rated capacity. For the example network considered, buses 10, 11 and 12 are the least desirable for PV
 218 connection without over loading any of the transmission lines (Figure 15). Based on this analysis, up
 219 to 110MW PV may be connected to any of the buses without any thermal violation.

220 For this example study, a PV capacity is acceptable if all the bus voltages are within 0.9-1.1pu,
 221 voltage differences with and without PV do not exceed 0.08pu for any bus, and the thermal loading
 222 for any of the transmission lines is below 100%. Study is primarily focused on PV penetrations
 223 without significant changes to existing infrastructure, therefore, supplementary devices such as
 224 voltage regulators, capacitor banks, and other complementary tools were not considered. This study
 225 demonstrates that the maximum PV capacity without any network violation depends on the PV POI
 226 (Figure 16). Based on the maximum PV capacity for the analyzed cases without voltage or thermal
 227 violations, the preferred PV POI for the analyzed network are buses 1,7 and 9.

228 7. Conclusion

229 This paper proposes an analytical framework, which includes a minute-to-minute economic
 230 dispatch model and a transmission network analyzing module for the evaluation of large solar PV
 231 impacts on both the generation and transmission systems. This framework can be employed for
 232 multiple applications including studies for estimating the maximum solar PV capacity a service
 233 area can support, the generation violations due to solar PV penetrations, the preferred location to
 234 connect solar PV plants, and the power system violations on the transmission network due to solar PV
 235 penetration. Furthermore, the proposed framework may be adopted for other intermittent sources
 236 such as wind power plants, and evaluate their effect on both the generation and transmission network
 237 system.

238 The detailed technical benefits for the proposed framework were demonstrated through the
 239 evaluation of the impact of increasing solar PV penetration on both the generation and transmission

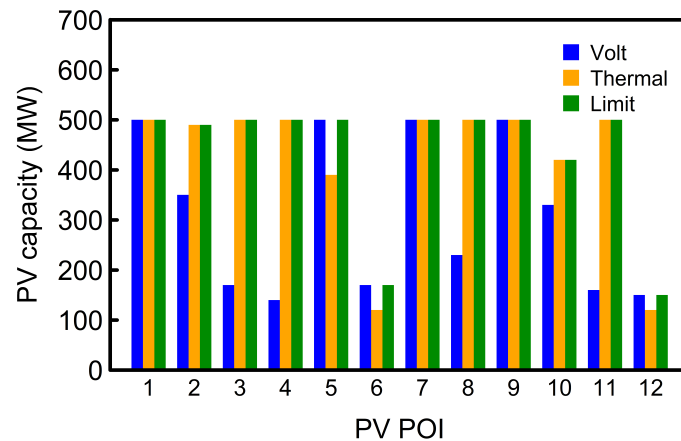


Figure 16. Maximum PV hosting capacity with respect to the circuit solution limit, voltage violation and thermal limits at peak load level.

240 network for a modified IEEE 12 bus system with four conventional generators. Contrary to
 241 conventional approaches based on hourly dispatch models, the proposed technique employs a detailed
 242 minute-to-minute economic dispatch model to capture the impact of increasing PV penetration and
 243 identify periods of generation imbalance suitable for regulatory practices. Additionally, the framework
 244 was used to estimate the maximum PV hosting capacity for the transmission network with regards to
 245 the bus voltage and transmission line violations.

246 Based on the results for the example transmission circuit and generators responses for the day
 247 evaluated, the maximum capacity of the solar PV plant a service area can sustain without needing
 248 significant upgrades to the existing infrastructure depends on, the available unit specifications, the PV
 249 point of interconnections, and the voltage and thermal limits of the transmission network buses and
 250 lines, respectively. The results from the example 2248 MW system evaluated indicate that the system
 251 can sustain up to 400 MW, 17.8% of capacity, PV penetration without substantial generation violation
 252 and up to 120 MW PV plant can be connected to any of the buses in the transmission network without
 253 any voltage or thermal violation at peak load. The hosting capacity of the transmission network
 254 considering solar PV plants at multiple POI and the integration of battery energy storage systems to
 255 improve the acceptable PV capacity on the circuit are subjects of ongoing studies.

256 Acknowledgment

257 The support of University of Kentucky, the L. Stanley Pigman endowment and of the Louisville
 258 Gas and Electric and Kentucky Utilities, part of the PPL Corporation family of companies is gratefully
 259 acknowledged.

260 **Author Contributions:** Conceptualization, Oluwaseun Akeyo, Aron Patrick and Dan M. Ionel; Formal
 261 analysis, Oluwaseun Akeyo; Funding acquisition, Aron Patrick; Investigation, Oluwaseun Akeyo; Methodology,
 262 Oluwaseun Akeyo, Aron Patrick and Dan M. Ionel; Supervision, Dan M. Ionel; Writing – original draft, Oluwaseun
 263 Akeyo; Writing – review & editing, Aron Patrick and Dan M. Ionel.

264 **Conflicts of Interest:** The authors declare no conflict of interest.

265

- 266 1. Blaabjerg, F.; Ionel, D.M. *Renewable energy devices and systems with simulations in MATLAB® and ANSYS®*;
 267 CRC Press, Boca Raton, FL, 2017.
- 268 2. Nelson, J.; Kasina, S.; Stevens, J.; Moore, J.; Olson, A.; Morjaria, M.; Smolenski, J.; Aponte, J. Investigating
 269 the economic value of flexible solar power plant operation. *Energy and Environmental Economics, Inc* **2018**.

- 270 3. Basu, M. Multi-region dynamic economic dispatch of solar–wind–hydro–thermal power system
271 incorporating pumped hydro energy storage. *Engineering Applications of Artificial Intelligence* **2019**,
272 *86*, 182–196.
- 273 4. Bai, J.; Ding, T.; Wang, Z.; Chen, J. Day-ahead robust economic dispatch considering renewable energy and
274 concentrated solar power plants. *Energies* **2019**, *12*, 3832.
- 275 5. Tavakoli, A.; Saha, S.; Arif, M.T.; Haque, M.E.; Mendis, N.; Oo, A.M.T. Impacts of grid integration of solar
276 PV and electric vehicle on grid stability, power quality and energy economics: a review. *IET Energy Systems*
277 *Integration* **2020**, *2*, 243–260.
- 278 6. Singhvi, V.; Ramasubramanian, D. Renewable generation hosting capacity screening tool for a transmission
279 network. Technical report, Electric Power Research Institute (EPRI), Knoxville, TN, 2018.
- 280 7. Jadoun, V.K.; Pandey, V.C.; Gupta, N.; Niazi, K.R.; Swarnkar, A. Integration of renewable energy sources
281 in dynamic economic load dispatch problem using an improved fireworks algorithm. *IET Renewable Power*
282 *Generation* **2018**, *12*, 1004–1011.
- 283 8. Singh, S.; Gao, D.W. Noiseless consensus based algorithm for economic dispatch problem in grid-connected
284 microgrids to enhance stability among distributed generators. 2019 North American Power Symposium
285 (NAPS). IEEE, 2019, pp. 1–5.
- 286 9. Kim, T.Y.; Won, G.H.; Chung, Y. Optimal dispatch and unit commitment strategies for multiple diesel
287 generators in shipboard power system using dynamic programming. 2018 21st International Conference
288 on Electrical Machines and Systems (ICEMS). IEEE, 2018, pp. 2754–2757.
- 289 10. Divshali, P.H.; Söder, L. Improving PV dynamic hosting capacity using adaptive controller for STATCOMs.
290 *IEEE Transactions on Energy Conversion* **2019**, *34*, 415–425.
- 291 11. Mahroo-Bakhtiari, R.; Izadi, M.; Safdarian, A.; Lehtonen, M. Distributed load management scheme to
292 increase PV hosting capacity in LV feeders. *IET Renewable Power Generation* **2020**, *14*, 125–133.
- 293 12. Diaz, D.; Kumar, A.; Deboever, J.; Grijalva, S.; Peppanen, J.; Rylander, M.; Smith, J. Scenario-selection
294 for hosting capacity analysis of distribution feeders with voltage regulation equipment. 2019
295 IEEE Power Energy Society Innovative Smart Grid Technologies Conference (ISGT), 2019, pp. 1–5.
296 doi:10.1109/ISGT.2019.8791586.
- 297 13. Le Baut, J.; Zehetbauer, P.; Kadam, S.; Bletterie, B.; Hatziargyriou, N.; Smith, J.; Rylander, M. Probabilistic
298 evaluation of the hosting capacity in distribution networks. 2016 IEEE PES Innovative Smart Grid
299 Technologies Conference Europe (ISGT-Europe), 2016, pp. 1–6. doi:10.1109/ISGTEurope.2016.7856213.
- 300 14. Feldman, D.J.; Margolis, R.M. Q4 2018/Q1 2019 Solar Industry Update. Technical report, National
301 Renewable Energy Lab.(NREL), Golden, CO (United States), 2019.
- 302 15. Crăciun, B.; Kerekes, T.; Séra, D.; Teodorescu, R.; Timbus, A. Benchmark networks for grid
303 integration impact studies of large PV plants. 2013 IEEE Grenoble Conference, 2013, pp. 1–6.
304 doi:10.1109/PTC.2013.6652114.
- 305 16. Khan, N.A.; Sidhu, G.A.S.; Gao, F. Optimizing combined emission economic dispatch for solar integrated
306 power systems. *IEEE Access* **2016**, *4*, 3340–3348.
- 307 17. Jadoun, V.K.; Pandey, V.C.; Gupta, N.; Niazi, K.R.; Swarnkar, A. Integration of renewable energy sources in
308 dynamic economic load dispatch problem using an improved fireworks algorithm. *IET Renewable Power*
309 *Generation* **2018**, *12*, 1004–1011.
- 310 18. Adamczyk, A.; Altin, M.; Göksu, .; Teodorescu, R.; Iov, F. Generic 12-bus test system for wind power
311 integration studies. 2013 15th European Conference on Power Electronics and Applications (EPE), 2013,
312 pp. 1–6. doi:10.1109/EPE.2013.6634758.
- 313 19. Live Solar Generation Data | LG&E and KU. Available online: <https://lge-ku.com/live-solar-generation>
314 (accessed on 10 Aug 2020).
- 315 20. Standard BAL-001-1 - Real power balancing control performance. *North American Electric Reliability*
316 *Corporation (NERC)*.
- 317 21. Standard BAL-002-1 - Real power balancing control performance. *North American Electric Reliability*
318 *Corporation (NERC)*.
- 319 22. Glover, J.D.; Sarma, M.S.; Overbye, T. *Power system analysis & design, SI version*; Cengage Learning, 2012.
- 320 23. Kokopeli, P.; Schreifels, J.; Forte, R. Assessment of startup period at coal-fired electric generating
321 units. *US Environmental Protection Agency, Office of Air and Radiation, technical report, Document ID:*

- 322 EPA-HQ-OAR-2009-0234-20378 [online] <http://www.epa.gov/airquality/powerplanttoxics/pdfs/matsstartstd.pdf>
323 (accessed 20 November 2013) **2013**.
- 324 24. Olowu, T.O.; Sundararajan, A.; Moghaddami, M.; Sarwat, A.I. Future challenges and mitigation methods
325 for high photovoltaic penetration: A survey. *Energies* **2018**, *11*, 1782.
- 326 25. IEEE Standard conformance test procedures for equipment interconnecting distributed energy resources
327 with electric power systems and associated interfaces. *IEEE Std 1547.1-2020* **2020**, pp. 1–282.
- 328 26. On FERC NOPR [Docket No. RM16-1-000] Proposal to revise standard generator interconnection
329 agreements. *North American Electric Reliability Corporation (NERC)*.

330 **Publisher's Note:** MDPI stays neutral with regard to jurisdictional claims in published maps and institutional
331 affiliations.

332 © 2021 by the authors. Submitted to *Energies* for possible open access publication under the terms and conditions
333 of the Creative Commons Attribution (CC BY) license (<http://creativecommons.org/licenses/by/4.0/>).